



СООБЩЕНИЯ
ОБЪЕДИНЕННОГО
ИНСТИТУТА
ЯДЕРНЫХ
ИССЛЕДОВАНИЙ

Дубна

95-444

E1-95-444

A.V.Bannikov, G.A.Chelkov, Z.K.Silagadze*

$B_s^0 \rightarrow D_s^- \alpha_1^+$ DECAY CHANNEL
IN THE B_s^0 -MIXING STUDIES

*Budker Institute of Nuclear Physics, 630090, Novosibirsk, Russia

1995

1 Introduction

The relativistic description of the deuteron has a long history. This problem still remains present although non-relativistic schemes of calculations are widely used to analyze reactions with the deuteron. There are different approaches which take into account relativistic effects. They can be separated into three groups: (i) the Bethe-Salpeter approach [1], (ii) a reduction of the Bethe-Salpeter equation (quasi-potential, light front dynamics), and (iii) prescriptive treatments.

The Bethe-Salpeter approach is the most consistent one. However, it contains some difficulties that do not allow to establish a direct link to the non-relativistic calculations – e.g. the absence of a non-relativistic reduction of arbitrary kernels or the problem to interpret the abnormal parity states.

Non-relativistic calculations with mesonic exchange currents give a reasonable description of the electromagnetic processes of the deuteron (e.g. elastic scattering and electrodisintegration). It is important to note that those *mesonic exchange currents treated in a non-relativistic framework* are partially included in the above mentioned relativistic calculations (i) and (ii) without additional assumptions. This has been demonstrated e.g. in Ref.[2] for the electrodisintegration of the deuteron in the formalism of light front dynamics.

Here, we present the investigation of a simple electromagnetic property of the deuteron, the magnetic moment, in the framework of the Bethe-Salpeter approach, and show the connection to the results of a non-relativistic calculation.

2 Basic definitions

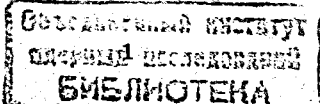
The main object of the Bethe-Salpeter approach is the vertex function $\Gamma(P, p)$ which obeys the Bethe-Salpeter equation, here written within the matrix formalism:

$$\Gamma(P, p) = i \int \frac{d^4 k}{(2\pi)^4} v(p, k) \Gamma^{(1)} S^{(1)} \left(\frac{P}{2} + k\right) \Gamma(P, k) \tilde{S}^{(2)} \left(\frac{P}{2} - k\right) \Gamma^{(2)}, \quad (1)$$

where $v(p, k) \Gamma^{(1)}$ $\otimes \Gamma^{(2)}$ is the interaction kernel, and $S^{(i)}$, $\tilde{S}^{(i)}$ are Feynman propagators. The vertex function for the deuteron can be decomposed into basis states of definite values of orbital momentum L , spin S and ρ -spin (Ref.[3, 4]). The general form in the rest frame is given by

$$\Gamma_M(P, p) = \sum_{\alpha} g_{\alpha}(p_0; |p|) \Gamma_M^{\alpha}(p), \quad (2)$$

where g_{α} are radial functions, and $\Gamma_M^{\alpha}(p)$ are spin – angular momentum parts.



1 Introduction

In the Standard Model B^0 and \bar{B}^0 are not mass eigenstates. Instead we have (the small CP-violating effects are neglected)

$$B^0 = \frac{B_1 + B_2}{\sqrt{2}}, \quad \bar{B}^0 = \frac{B_1 - B_2}{\sqrt{2}}. \quad (1)$$

So the time evolution of the B_i states looks like

$$B_i(t) = B_i(0) \exp \left\{ -\frac{i}{\hbar} (m_i - i \frac{\Gamma_i}{2}) t \right\}, \quad (2)$$

where m_i is the mass eigenvalue and Γ_i - the corresponding width.

It follows from (1) and (2) that the probability for B^0 meson not to change its flavour after a time t from the creation is

$$P^{B^0 B^0}(t) = |\langle B^0(t) | B^0(0) \rangle|^2 = \frac{1}{2} e^{-\frac{\Gamma t}{\hbar}} \left(\cosh \frac{\Delta \Gamma t}{2\hbar} + \cos \frac{\Delta m t}{\hbar} \right), \quad (3)$$

and the probability to convert into the \bar{B}^0 meson -

$$P^{B^0 \bar{B}^0}(t) = |\langle \bar{B}^0(t) | B^0(0) \rangle|^2 = \frac{1}{2} e^{-\frac{\Gamma t}{\hbar}} \left(\cosh \frac{\Delta \Gamma t}{2\hbar} - \cos \frac{\Delta m t}{\hbar} \right), \quad (4)$$

where $\Gamma = \frac{1}{2}(\Gamma_1 + \Gamma_2)$ is the average width and $\Delta \Gamma = \Gamma_1 - \Gamma_2$. So $\Delta m = m_1 - m_2$ mass difference between the B mass eigenstates defines the oscillation frequency. Standard Model predicts [1] that $\frac{\Delta m_s}{\Delta m_d} \sim \left| \frac{V_{ts}}{V_{td}} \right|^2 \gg 1$, V_{ij} being the Cabibbo-Kobayashi-Maskawa matrix element. Therefore the mixing in the B_s^0 meson system proceeds much more faster than in the B_d^0 system.

The total probability χ that a B^0 will oscillate into \bar{B}^0 is

$$\chi = \int_0^\infty P^{B^0 \bar{B}^0}(t) \frac{dt}{\tau} (1 - y^2) = \frac{1}{2} \left(\frac{x^2}{1+x^2} + \frac{y^2}{1-y^2} \right) (1 - y^2), \\ x = \frac{\Delta m}{\Gamma}, \quad y = \frac{\Delta \Gamma}{2\Gamma}. \quad (5)$$

In the first B_d -mixing experiments [2] just this time integrated mixing probability was measured. The result [3] $x_d = 0.69 \pm 0.07$ shows that in the B_s system $x_s \gg 1$ is expected. In fact the allowed range of x_s is estimated to be between ~ 12 and ~ 30 in the Standard Model [4]. Such a big value of x_s makes impossible time integrated measurements in the B_s system, because χ in (5) saturates at ~ 0.5 for large values of x .

Although it was thought that unlike the kaon system for the B mesons the decay width difference can be neglected [5], nowadays people is more inclined to believe

the theoretical prediction [6] that the $b \rightarrow c\bar{s}$ transition, with final states common to both B_s and \bar{B}_s , can generate about 20% difference in lifetimes of the short lived and long lived B_s -mesons [7].

But we can see from the (3 ÷ 5) formulas that the effect of nonzero y is always $\sim y^2$ and so of the order of several percents, because $y \approx 0.1$ is expected. In the following we will neglect this effect and will take $y = 0$, though in some formulas y is kept for reference reason.

The development of high precision vertex detectors made it possible to measure [8] in the B_d system the time dependent asymmetry

$$\frac{P^{B^0 B^0} - P^{B^0 \bar{B}^0}}{P^{B^0 B^0} + P^{B^0 \bar{B}^0}} = \cos \frac{\Delta m t}{\hbar} . \quad (6)$$

The same technics can be applied to the $B_s - \bar{B}_s$ system also.

Recently the ATLAS detector sensitivity to the x_s parameter was studied [9] using $B_s^0 \rightarrow D_s^- \pi^+ \rightarrow \phi \pi^- \pi^+ \rightarrow K^+ K^- \pi^- \pi^+$ decay chain for B_s meson reconstruction. It was shown that x_s up to 40 should be within a reach [10]. The signal statistics could be increased by using other decay channels, like $B_s^0 \rightarrow D_s^- a_1^+$, $B_s^0 \rightarrow J/\Psi K^* 0$.

The purpose of this note is to study the usefulness of the decay chain $B_s^0 \rightarrow D_s^- a_1^+ \rightarrow \phi \pi^- \rho \pi^+ \rightarrow K^+ K^- \pi^- \pi^+ \pi^- \pi^+$ for B_s meson reconstruction in the ATLAS B_s -mixing experiments.

2 Event simulation

About 20 000 following b-decays were generated using the PYTHIA Monte Carlo program [11]

$$(p_T^\mu > 6 \text{ GeV}/c, |\eta^\mu| < 2.2) \quad \mu_{tag} \leftarrow \bar{b}\bar{b} \rightarrow B_s^0 \rightarrow D_s^- a_1^+ \rightarrow \begin{aligned} &\rightarrow \rho^0 \pi^+ \\ &\rightarrow \pi^+ \pi^- \\ &\rightarrow \phi \pi^- \\ &\rightarrow K^+ K^- \end{aligned}$$

The impact parameter was smeared using the following parameterized description of the impact parameter resolution

$$\sigma_{IP} = 14 \oplus 72/(p_T \sqrt{|\sin \theta|}) \quad \sigma_Z = 20 \oplus 83/(p_T \sqrt{|\sin \theta|^3}) , \quad (7)$$

where resolutions are in μm and θ is the angle with respect to the beam line. It was shown in [9] that this parameterized resolution reasonably reproduces the results obtained by using the full simulation and reconstruction programs.

For the transverse momentum resolution an usual expression [10]

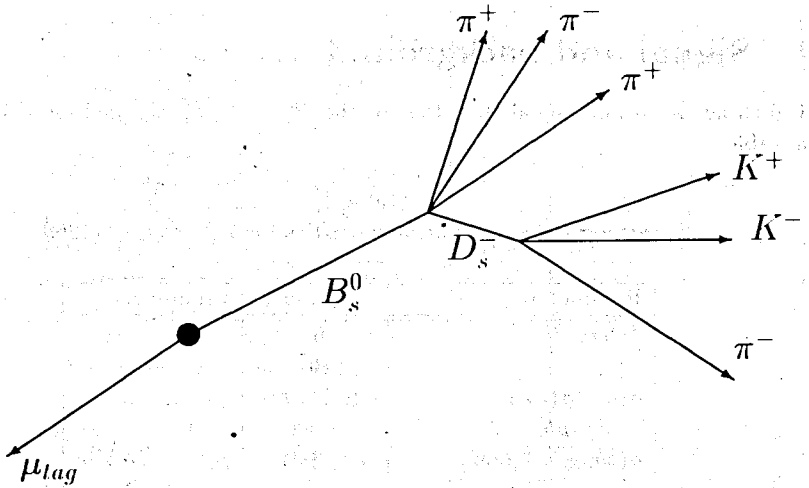
$$\frac{\sigma(p_T)}{p_T} = 5 \cdot 10^{-4} p_T \pm 1.2\% \quad (8)$$

was assumed.

Track reconstruction efficiencies for various particles were taken from [10]. Because now we have 6 particles in the final state instead of 4 for the $B_s^0 \rightarrow D_s^- \pi^+$ decay channel, we expect some loss in statistics due to track reconstruction inefficiencies, but the effect is not significant because the investigation in [10] indicates a high reconstruction efficiency of 0.95.

3 Event reconstruction

The topology of a considered B_s^0 decay chain is shown schematically in a figure:



The B_s decay vertex reconstruction was done in the following three steps.

First of all the D_s^- was reconstructed by finding three charged particles presumably originated from the D_s^- decay and fitting their tracks. For this goal all combinations of the properly charged particles were examined in the generated events assuming that two of them are kaons and one is pion. The resulting invariant mass distribution is shown in Fig. 1a. The expected D_s^- peak is clearly seen along

with moderate enough combinatorial background. Cuts on $\Delta\phi_{KK}$, $\Delta\theta_{KK}$ and $|M_{KK} - M_\phi|$ were selected in order to optimize signal to background ratio. To select one more cut on $|M_{KK\pi} - M_{D_s^-}|$, the information about the invariant mass resolution is desirable. Fig. 2a shows the reconstructed D_s^- meson from its true decay products. The finite invariant mass resolution is due to applied track smearing and equals approximately to $10\text{ MeV}/c^2$.

After D_s^- meson reconstruction, a_1^+ meson was searched in three particle combinations from the remaining charged particles, each particle in the combination being assumed to be a pion. Fig. 1b shows a resulting invariant mass distribution. Because of huge width of a_1^+ , signal to background separation is not so obvious in this case. If a_1^+ is reconstructed from its true decay products as in Fig. 2b, its width is correctly reproduced. To draw out a_1^+ from the background, further cuts were applied on $\Delta\phi_{\pi\pi}$, $\Delta\theta_{\pi\pi}$, $|M_{\pi\pi} - M_\rho|$ and $|M_{\pi\pi\pi} - M_{a_1}|$.

At last B_s^0 decay vertex was fitted, using reconstructed D_s^- and a_1^+ .

Almost the same resolution in the B_s -decay proper time was reached $\sigma_\tau \approx 0.064\text{ ps}$, as in [9]. The corresponding resolution in the B-meson decay length in the transverse plane is $\approx 87\mu\text{m}$. The relevant distributions are shown in Fig.3.

4 Signal and background

Branching ratios and signal statistics for the $B_s^0 \rightarrow D_s^- a_1^+$ channel are summarized in Table 1.

Table 1.

Branching ratios and signal statistics for $B_s^0 \rightarrow D_s^- a_1^+(1260)$.

Parameter	Value	Comment
$L [\text{cm}^{-2}\text{s}^{-1}]$	10^{33}	
$t [\text{s}]$	10^7	
$\sigma(bb)/\sigma(\text{tot})$	$\simeq 1/100$	
$\sigma(bb) [\mu\text{b}]$	$\simeq 500$	
$\sigma(bb \rightarrow \mu X) [\mu\text{b}]$	$\simeq 2.24$	$p_T^\mu > 6\text{ GeV}/c$, $ \eta^\mu < 2.2$
$N(bb \rightarrow \mu X)$	2.24×10^{10}	
$Br(b \rightarrow B_s^0)$	0.1	
$Br(B_s^0 \rightarrow D_s^- a_1^+)$	0.006	
$Br(D_s^- \rightarrow \phi\pi^-)$	0.035	
$Br(\phi \rightarrow K^+K^-)$	0.491	
$Br(a_1^+ \rightarrow \rho^0\pi^+)$	~ 0.5	
$Br(\rho^0 \rightarrow \pi^-\pi^+)$	~ 1	
$N(K^+K^-\pi^+\pi^-\pi^+)$	116000	

Note that we use an updated value for $\text{Br}(D_s^- \rightarrow \phi\pi^-)$ from [12]. B_s^0 branching ratios are still unknown experimentally. Neglecting SU(3) unitary symmetry breaking effects, we have taken $\text{Br}(B_s^0 \rightarrow D_s^- a_1^+) \approx \text{Br}(B^0 \rightarrow D^- a_1^+)$.

Acceptance and analysis cuts are summarized in Table 2. We take a track reconstruction efficiency of 95% and a lepton identification efficiency of 80%, as in [10].

Table 2.

Analysis cuts and acceptance for $B_s^0 \rightarrow D_s^- a_1^+(1260)$ (for 10^4 pb^{-1} integrated luminosity).

Parameter	Value	Comment
$N(K^+K^-\pi^+\pi^-\pi^+)$	116000	
Cuts :		
$p_T > 1\text{ GeV}/c$		
$ \eta < 2.5$		
$N(K^+K^-\pi^+\pi^-\pi^+)$	7680	6.6%
$\Delta\varphi_{KK} < 10^\circ$		
$\Delta\theta_{KK} < 10^\circ$		
$ M_{KK} - M_\phi < 20\text{ MeV}/c^2$		
$ M_{KK\pi} - M_{D_s^-} < 15\text{ MeV}/c^2$		
$\Delta\varphi_{\pi\pi} < 35^\circ$		
$\Delta\theta_{\pi\pi} < 15^\circ$		
$ M_{\pi\pi} - M_{\rho^0} < 192\text{ MeV}/c^2 (\pm 3\sigma)$		
$ M_{\pi\pi\pi} - M_{a_1^+} < 300\text{ MeV}/c^2$		
$N(K^+K^-\pi^+\pi^-\pi^+)$	5765	5.0%
D_s^- vertex fit $\chi^2 < 12.0$		
a_1^+ vertex fit $\chi^2 < 12.0$		
B_s^0 vertex fit $\chi^2 < 0.35$		
B_s^0 proper decay time $> 0.4\text{ ps}$		
B_s^0 impact parameter $< 55\mu\text{m}$		
B_s^0 $p_T > 10.0\text{ GeV}/c$		
$N(K^+K^-\pi^+\pi^-\pi^+)$ after cuts	3505	3.0%
Lepton identification	0.8	
Track efficiency	$(0.95)^6$	
$N(K^+K^-\pi^+\pi^-\pi^+)$ reconstructed	2065	1.8%

As we see, about 2065 reconstructed B_s^0 are expected after one year run at $\mathcal{L} = 10^{33}\text{ cm}^{-2}\text{s}^{-1}$ luminosity. The corresponding number of events within one standard deviation ($\simeq 22\text{ MeV}/c^2$) from the B_s^0 mass equals 1407. This last number should be compared to 2650 signal events, as reported in [10], then $B_s^0 \rightarrow D_s^- \pi^+$ decay channel is used.

Events which pass the first level muon trigger ($p_T > 6 \text{ GeV}/c$, $|\eta| < 2.2$) are predominantly $b\bar{b}$ events. Background can come from other B decays of the same or higher charged multiplicity, and from random combinations with some (or all) particles originating not from a B decay (combinatorial background).

The following channels were considered and no significant contributions were found to the background:

- $B_d^0 \rightarrow D_s^- a_1^+$. These events don't pass the analysis cuts, because the D_s^- mass is shifted from the D_s^- mass by about 100 MeV, and so does the B_d^0 mass compared to the B_s^0 mass.
- $\Lambda_b \rightarrow \Lambda_c^+ \pi^-$, followed by $\Lambda_c^+ \rightarrow p K^- \pi^+ \pi^+ \pi^-$. Taking $Br(\Lambda_b \rightarrow \Lambda_c^+ \pi^-) \approx 0.01$ from [13], we see that the expected number of $pK4\pi$ events, originated from this source, is only five times less than the expected number of truly signal events. But the decay topology for this decay chain is drastically different (1+5, not 3+3) and therefore it is unexpected that significant amount of the B -decays will be simulated in this way.

Note that even for $B_s \rightarrow D_s^- \pi^+$ decay channel the similar background is negligible [9], although $Br(\Lambda_c^+ \rightarrow p K^- \pi^+)$ is about 44 times bigger than $Br(\Lambda_c^+ \rightarrow p K^- \pi^+ \pi^+ \pi^-)$.

- $B_d^0 \rightarrow D_s^- a_1^+$. About 10 000 such events were generated by PYTHIA and then analyzed. Using $Br(B_d^0 \rightarrow D_s^+ a_1^-) < 2.7 \cdot 10^{-3}$ from [12] and assuming that $B_d^0 \rightarrow D_s^- a_1^+$ decay goes through $B^0 \bar{B}^0$ oscillations: $B_d^0 \rightarrow B_d^0 \rightarrow D_s^- a_1^+$, and therefore $Br(B_d^0 \rightarrow D_s^- a_1^+) = \chi_d Br(B_d^0 \rightarrow D_s^+ a_1^-) < 4.3 \cdot 10^{-4}$, we have got Fig.4. It is seen from this figure that because of $M_{B_s} - M_{B_d} \approx 100 \text{ MeV}$ mass shift, the contribution of this channel to the background proves to be negligible.

Note that Fig.4 refers to the total number of the $B_d^0 \rightarrow D_s^- a_1^+$ events. In fact the distribution of these events with regard to the decay proper time is oscillatory, x_d (not x_s) defining the oscillation frequency. So in general this will result in oscillatory dilution factor. The conclusion that this dilution factor is irrelevant relies on the fact that no candidate event was found with invariant mass within one standard deviation from the B_s mass for $6 \cdot 10^4 \text{ pb}^{-1}$ integrated luminosity.

A huge Monte-Carlo statistics is needed for combinatorial background studies. No candidate event with $M_{B_s^0} - 150 \text{ MeV}/c^2 < M_{KK\pi\pi\pi} < M_{B_s^0} + 150 \text{ MeV}/c^2$ was found within $\sim 3 \cdot 10^5$ inclusive μX events. This indicates that signal/background ratio is expected to be not worse than 1:1.

5 Dilution factors

The observation of the $B - B$ oscillations is complicated by some dilution factors. First of all the decay proper time is measured with some accuracy σ . From previous discussions we know that in our case $\sigma = 0.06 \text{ ps}$ is expected. Due to this finite time resolution, the observed oscillations are convolutions of the expressions (3) and (4) given above with a Gaussian distribution. For example

$$P^{B^0 B^0} \rightarrow \frac{1}{2} \int_{-\infty}^{\infty} e^{-\frac{t-s}{\sigma}} \left(\cosh \frac{\Delta \Gamma t}{2h} - \cos \frac{\Delta m s}{h} \right) \exp \left[-\frac{(t-s)^2}{2\sigma^2} \right] \frac{ds}{\sqrt{2\pi}\sigma} \sim \\ \frac{1}{2} e^{-\frac{t}{\tau}} \left(\cosh \frac{\Delta \Gamma}{2h}(t - \sigma \frac{\sigma}{\tau}) - D_{time} \cos \frac{\Delta m}{h}(t - \sigma \frac{\sigma}{\tau}) \right) \quad (9)$$

where $D_{time} = \exp \left[-\frac{1}{2} \left(\frac{\sigma}{\tau} \right)^2 (x^2 + y^2) \right]$, $\tau = \frac{h}{\Gamma}$.

So the main effect of this smearing is the reduction of the oscillation amplitude by D_{time} . This is quite important in the B_s system where $x \gg 1$. There is also a time shift $t \rightarrow t - \sigma \frac{\sigma}{\tau}$ in (9). This time shift does not really effect the observability of the oscillations and we will neglect it.

In fact (9) is valid only for not too short decay times $t \gg \sigma$, because in (3) and (4) distributions $t > 0$ is assumed.

Another reduction in the oscillation amplitude is caused by the particle/antiparticle mistagging at $t=0$. In our case, particle/antiparticle nature of the B -meson is tagged by the lepton charge in the semileptonic decay of the associated beauty hadron. Mistagging is mainly due to

- $B - B$ oscillations: accompanying b-quark can be hadronized as a neutral B meson and oscillate into B before semileptonic decay.
- $b \rightarrow c \rightarrow l^+$ cascade process, then the lepton is misidentified as having come directly from the B -meson and associated to the $b \rightarrow l^+$ decay.
- leptons coming from other decaying particles (K, π, \dots).
- detector error in the lepton charge identification.

Let η be the mistagging probability. If we have tagged N B^0 mesons, among them only $(1 - \eta)N$ are indeed B^0 -s and ηN are B^0 -s misidentified as B^0 -s. So at the proper time t we would observe $(P^{B^0 B^0}(t) = P^{B^0 B^0}(t))$ due to CPT invariance

$$N \left[(1 - \eta) P^{B^0 B^0}(t) + \eta P^{B^0 B^0}(t) \right] = \frac{N}{2} e^{-\frac{t}{\tau}} \left[\cosh \frac{\Delta \Gamma t}{2h} - (1 - 2\eta) \cos \frac{\Delta m t}{h} \right]$$

decays associated to the B^0 meson and therefore

$$P^{B^0 B^0}(t) \rightarrow \frac{1}{2} e^{-\frac{t}{\tau}} \left[\cosh \frac{\Delta \Gamma t}{2h} - (1 - 2\eta) \cos \frac{\Delta m t}{h} \right] .$$

So the dilution factor due to mistagging is $D_{tag} = 1 - 2\eta$. In our studies we have taken $D_{tag} = 0.56$, as in [14].

Finally the dilution can emerge from background. Suppose that apart from

events with $B \rightarrow B$ oscillations we also have $N_{back}(t)$ additional background events. Half of them will simulate \bar{B} meson and half of them B meson (assuming asymmetry free background). So the observed number of would be $B \rightarrow \bar{B}$ oscillations will be

$$\frac{N_{signal}}{2} e^{-\frac{\Gamma t}{h}} \left(\cosh \frac{\Delta \Gamma t}{2h} - \cos \frac{\Delta m t}{h} \right) + \frac{N_{back}(t)}{2} \sim e^{-\frac{\Gamma t}{h}} \left(\cosh \frac{\Delta \Gamma t}{2h} - D_{back} \cos \frac{\Delta m t}{h} \right)$$

and the oscillation amplitude will be reduced by an amount

$$D_{back} = \frac{N_{signal} \cdot \cosh \frac{\Gamma t}{\tau}}{N_{signal} + N_{back}(t) e^{\frac{\Gamma t}{\tau}}}.$$

Neglecting the proper time dependence of this dilution factor (that is supposing that the background is mainly due to B -hadron decays and therefore has approximately the same proper time exponential decay as the signal [15]), we have taken $D_{back} \approx 0.71$ which corresponds to the 2:1 signal/background ratio.

6 Prospects for x_s measurements

For $6 \cdot 10^4 pb^{-1}$ integrated luminosity the number of reconstructed B_s^0 -s would reach ~ 8000 from the analyzed channel alone. Another ~ 16000 B_s^0 -s are expected from the $B_s^0 \rightarrow D_s^- \pi^+$ channel [9, 10].

For events in which B_s^0 meson does not oscillate before its decay, the D_s meson and the tagging muon have equal sign charges. If the B_s^0 -meson oscillates, opposite charge combination emerges. The corresponding decay time distributions are

$$\begin{aligned} \frac{dn(++)}{dt} &= \frac{N}{2\tau} e^{-\frac{t}{\tau}} \left(1 + D \cos \left(\frac{x_s t}{\tau} \right) \right) \\ \frac{dn(+-)}{dt} &= \frac{N}{2\tau} e^{-\frac{t}{\tau}} \left(1 - D \cos \left(\frac{x_s t}{\tau} \right) \right) \end{aligned} \quad (10)$$

D is the product of all dilution factors and N is the total number of reconstructed B_s^0 -s.

The unification of samples from $B_s^0 \rightarrow D_s^- a_1^+$ and $B_s^0 \rightarrow D_s^- \pi^+$ decay channels allows to increase x_s measurement precision.

Fig.7 and Fig.8 show the corresponding

$$A(t) = \frac{\frac{dn(++)}{dt} - \frac{dn(+-)}{dt}}{\frac{dn(++)}{dt} + \frac{dn(+-)}{dt}} = D \cos \left(\frac{x_s t}{\tau} \right)$$

asymmetry plots for $x_s = 20$ and 35.

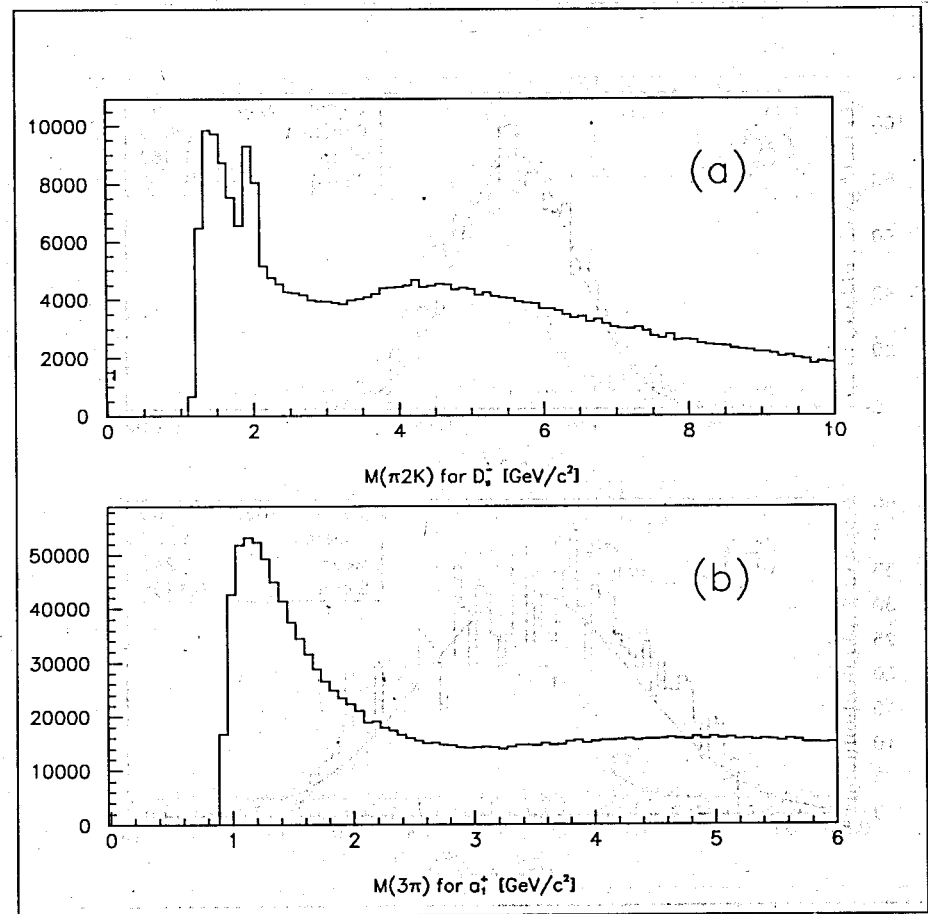


Figure 1: Invariant mass distributions of three charge particle combinations, assuming $2K + \pi$ (a) or 3π combination (b) as described in the text.

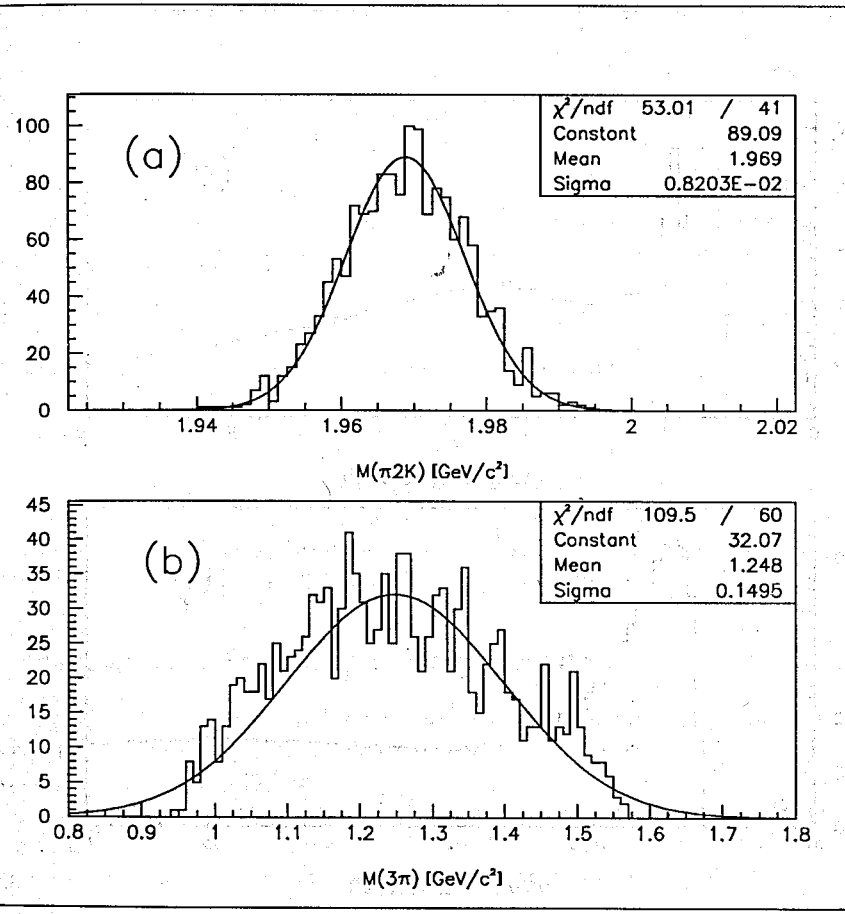


Figure 2: Three particle invariant mass distributions of reconstructed D_s^- a events.

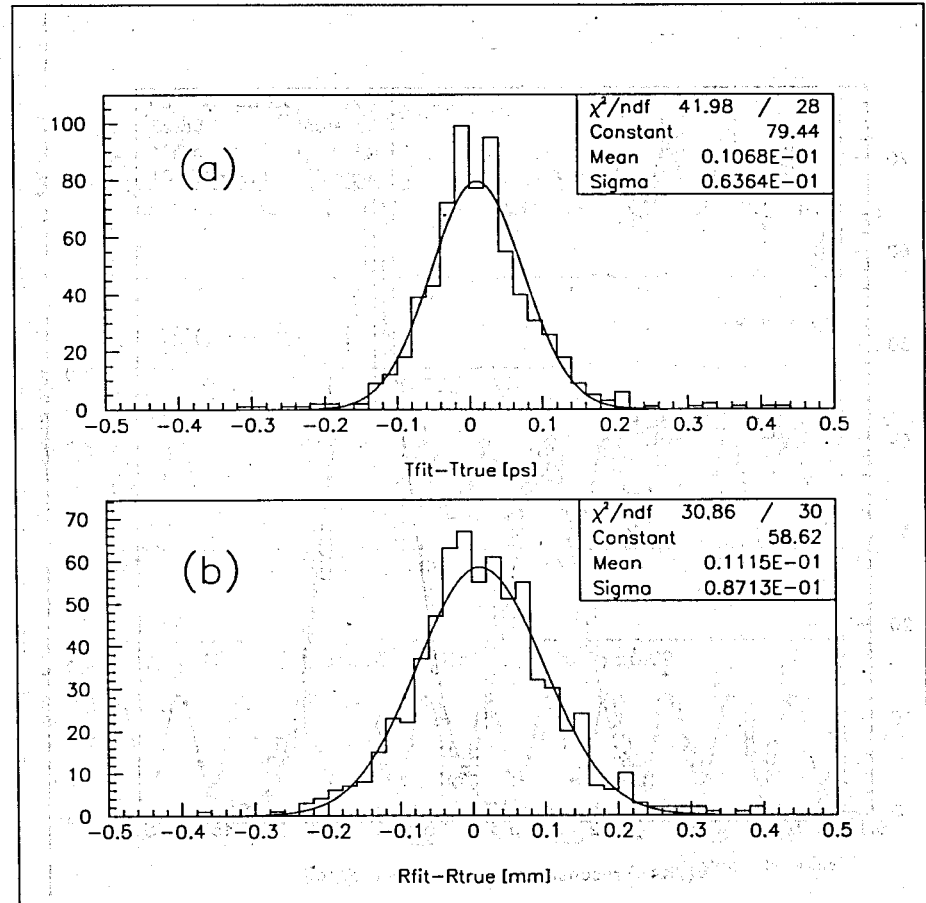


Figure 3: Proper time (a) and transverse radius (b) resolutions for the reconstructed B_s^0 decay vertex.

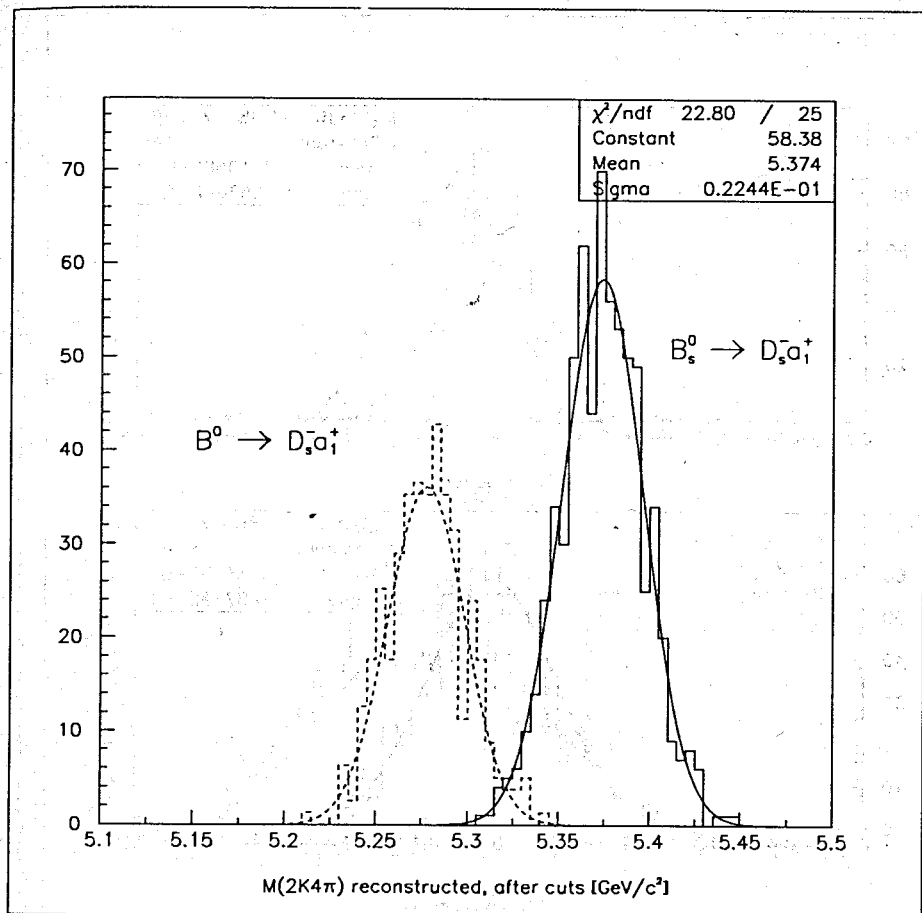


Figure 4: Six particle invariant mass distribution corresponding to the B_s^0 meson. Dashed line - expected upper limit for background from B^0 decay.

12

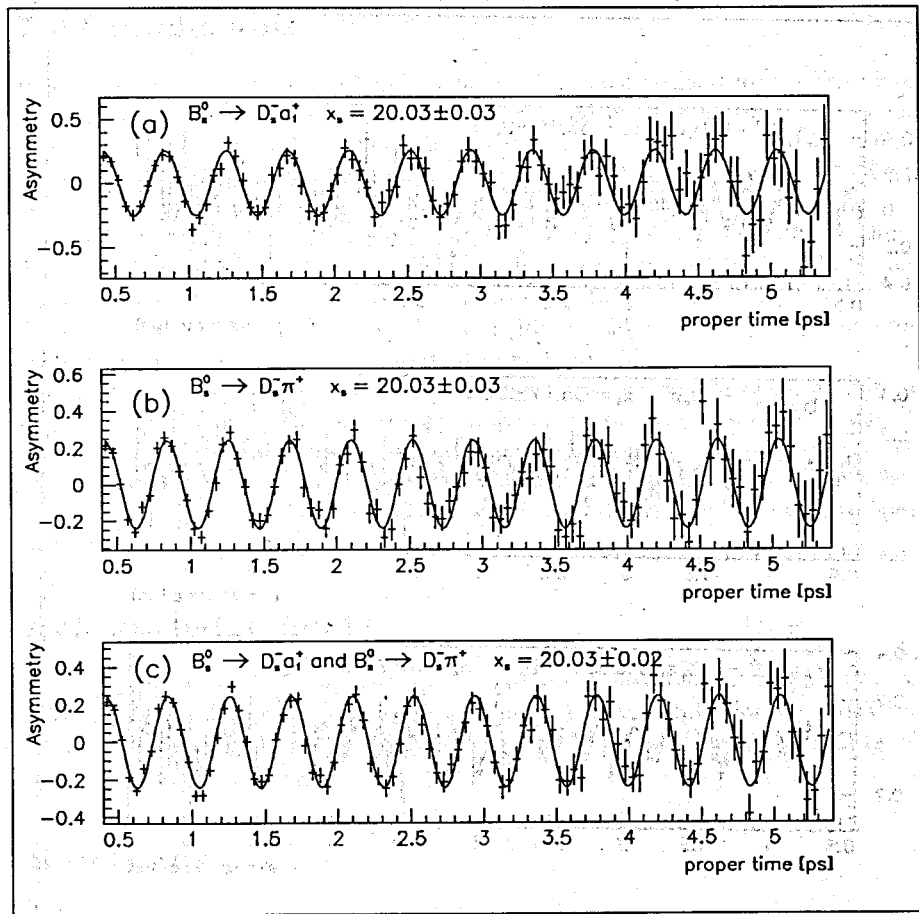


Figure 5: Asymmetry distributions for $B_s^0 \rightarrow D_s^- a_1^+$ (a); $B_s^0 \rightarrow D_s^- \pi^+$ (b) and when both channels are used (c), for $x_s = 20$.

13

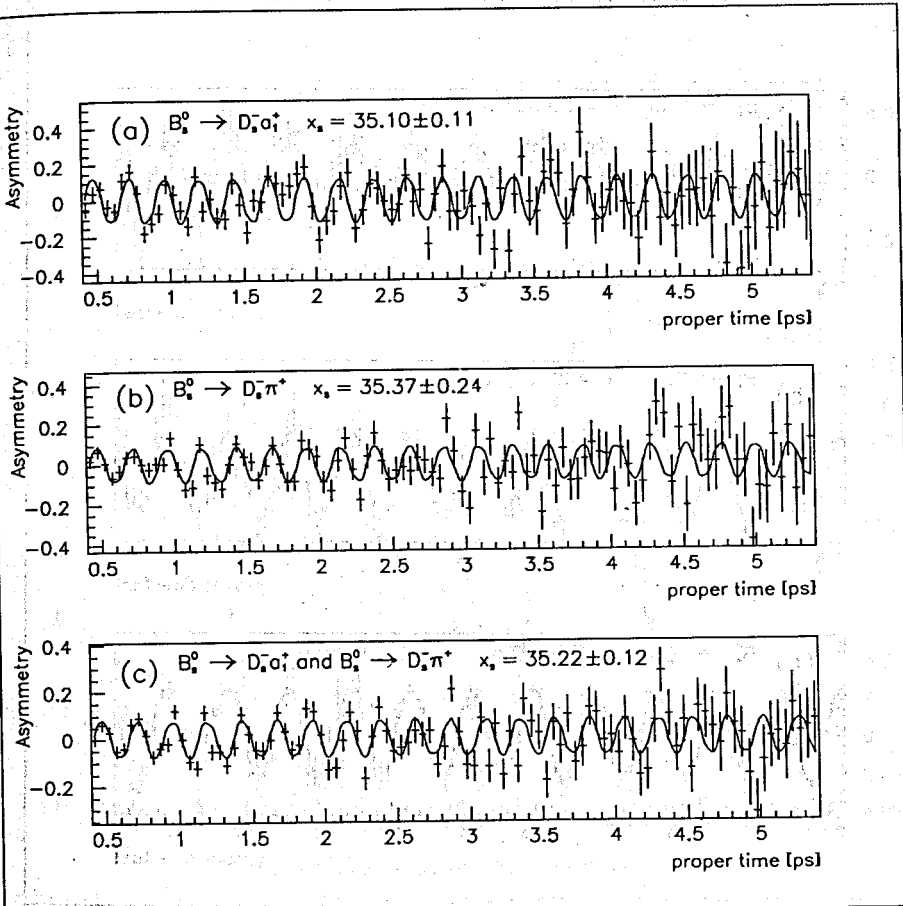


Figure 6: Asymmetry distributions for $B_s^0 \rightarrow D_s^- a_1^+$ (a), $B_s^0 \rightarrow D_s^- \pi^+$ (b) and when both channels are used (c), for $x_s = 35$.

7 Conclusions

It seems to us that $B_s^0 \rightarrow D_s^- a_1^+$ decay channel is almost as good for the B_s -mixing exploration as previously studied $B_s^0 \rightarrow D_s^- \pi^+$ and enables us to increase signal statistics about 1.5 times. Further gain in signal statistics can be reached [9, 10] by using $B_s^0 \rightarrow J/\psi K^*$ decay mode and considering other decay channels of D_s^- . These possibilities are under study.

We refrain from giving any particular value of x_s as an attainable upper limit. Too many uncertainties are left before a real experiment will start. Note, for example, that about two times bigger branching ratios for both $B_s \rightarrow D_s^- \pi^+$ and $B_s \rightarrow D_s^- a_1^+$ decay channel are predicted in [16], $\sim 500\mu b$ as a bb production cross section can also have significant variation in real life [17].

So although the results of this investigation strengthen confidence in reaching x_s as high as 40 [10], it should be realized that some theoretical predictions about B_s -physics and collider operation were involved and according to T.D.Lee's first law of physicist [18] "without experimentalist, theorist tend to drift". However maybe it is worthwhile to recall his second law also "without theorist, experimentalists tend to falter".

Acknowledgements

Many suggestions of P.Eerola strongly influenced this investigation and lead to considerable improvement of the paper. Communications with S.Gadomski and N.Ellis are also appreciated. Authors thank N.V. Makhaldiani for drawing their attention to T.D.Lee's paper.

References

- [1] A. Ali, D. London, J. Phys. **G19** (1993), 1069.
- [2] see for example:
UA1 Coll., H.C. Albajar et al., Phys. Lett. **B186** (1987), 217; **262** (1991), 171.
CLEO Coll., J. Bartelt et al., Phys. Rev. Lett. **71** (1993), 1680.
ARGUS Coll., H. Albrecht et al., Z. Phys. **C55** (1992), 357.
ALEPH Coll., D. Buskulic et al., Phys. Lett. **284** (1992), 177.
OPAL Coll., P.D. Acton et al., Phys. Lett. **B276** (1992), 379.
L3 Coll., B. Adeva et al., Phys. Lett. **B288** (1992), 395.
DELPHI Coll., P. Abreu et al., Phys. Lett. **B332** (1994), 488.
- [3] H.-G. Moser, B-mixing. Talk given at the 5th International Symposium on Heavy Flavour Physics, Montreal, Canada, 1993. CERN-PPE/93-164.

- [4] A. Ali, D. London, CP violation and flavour mixing in the Standard Model, DESY-95-148 (hep-ph/9508272).
- A. Ali, D. London, Implications of the top quark mass measurement for the CKM parameters, x_s , and CP asymmetries, CERN-TH.7398/94 (hep-ph/9408332).
- [5] A.J. Buras, W. Slominsski, H. Steger , Nucl. Phys. **B245** (1984), 369.
- P.J. Franzini, Phys. Rep. **173** (1989), 1.
- [6] M.B. Voloshin et al., Yad. Fiz. **46** (1987), 181.
- A. Datta, E.A. Paschos, U. Türke, Phys. Lett. **B196** (1987), 382.
- [7] L.I. Bigi, Lifetimes of heavy-flavour hadrons - whence and whither? UND-IIHEP-95-BIG06 (hep-ph/9507364).
- I. Dunietz: $B_s - B_s$ mixing, CP violation and extraction of CKM phases from untagged B_s data samples, FERMILAB-PUB-94/361-T (hep-ph/9501287).
- [8] ALEPII Coll., D. Decamp et al., Phys. Lett. **B313** (1993), 498.
- ALEPH Coll., D. Buskulic et al., CERN-PPE/93-99 .
- OPAL Coll., R. Akers et al., CERN-PPE/94-43 .
- [9] P. Eerola, S. Gadomski, B. Murray , B_s^0 -mixing measurement in ATLAS, ATLAS Internal Note PHYS-NO-039, 1994.
- [10] ATLAS technical proposal , CERN/LHCC/94-43 ,1994. p.255.
- [11] T.Sjöstrand, PYTHIA 5.7 and JETSET 7.4 : physics and manual, CERN-TH.7112/93, 1993.
- [12] Review of Particle Properties , Phys. Rev. **D50**, 1994.
- [13] S. Rudaz, M.B. Voloshin, Phys. Lett. **B252** (1990), 443.
- [14] P. Eerola et al. , Asymmetries in B decays and their experimental control, ATLAS Internal Note PHYS-NO-054, 1994 .
- [15] P. Camarri, A. Nisati , Time-dependent analysis of CP-asymmetries in the $B_d^0 B_d^0$ system, ATLAS Internal Note PHYS-NO-065, 1995 .
- [16] P. Blasii, P. Colangelo, G. Nandulli, Phys. Lett. **B283**(1992), 434.
- [17] P. Eerola, Measurement of CP-violation in B-decays with the ATLAS experiment, ATLAS Internal Note, PHYS-NO-009, 1992.
- [18] T. D. Lee, The evolution of weak interactions, Talk given at the symposium dedicated to Jack Steinberger, Geneva, 1986, CERN 86-07.

Received by Publishing Department
on October 26, 1995.

In order to exhibit the ρ -spin dependence, the spin - angular momentum functions $\Gamma_M^\alpha(p)$ may be replaced via $\Gamma_M^\alpha(p) \equiv \Gamma_M^{\tilde{\alpha}, \rho_1 \rho_2}(p)$, where

$$\begin{aligned}\Gamma_M^{\tilde{\alpha}, ++}(p) &= \frac{m + \hat{p}_2}{\sqrt{2E(m+E)}} \frac{1 + \gamma_0}{2} \tilde{\Gamma}_M^{\tilde{\alpha}}(p, \xi) \frac{m - \hat{p}_1}{\sqrt{2E(m+E)}}, \\ \Gamma_M^{\tilde{\alpha}, --}(p) &= \frac{m - \hat{p}_1}{\sqrt{2E(m+E)}} \frac{-1 + \gamma_0}{2} \tilde{\Gamma}_M^{\tilde{\alpha}}(p, \xi) \frac{m + \hat{p}_2}{\sqrt{2E(m+E)}}, \\ \Gamma_M^{\tilde{\alpha}, +-}(p) &= \frac{m + \hat{p}_2}{\sqrt{2E(m+E)}} \frac{1 + \gamma_0}{2} \tilde{\Gamma}_M^{\tilde{\alpha}}(p, \xi) \frac{m + \hat{p}_2}{\sqrt{2E(m+E)}}, \\ \Gamma_M^{\tilde{\alpha}, -+}(p) &= \frac{m - \hat{p}_1}{\sqrt{2E(m+E)}} \frac{1 - \gamma_0}{2} \tilde{\Gamma}_M^{\tilde{\alpha}}(p, \xi) \frac{m - \hat{p}_1}{\sqrt{2E(m+E)}}.\end{aligned}\quad (3)$$

with $\tilde{\alpha} \in \{L, S, J\}$, m is the nucleon mass, $\hat{p} = \gamma_\mu p^\mu$, and $\tilde{\Gamma}_M^{\tilde{\alpha}}$ given by

$$\begin{array}{c|c}\tilde{\alpha} & \frac{\sqrt{8\pi}}{\xi_M} \tilde{\Gamma}_M^{\tilde{\alpha}} \\ \hline ^3S_1 & \xi_M \\ ^3D_1 & -\frac{1}{\sqrt{2}} \left[\hat{\xi}_M + \frac{3}{2}(\hat{p}_1 - \hat{p}_2)(p\xi_M)|p|^{-2} \right] \\ ^3P_1 & \sqrt{\frac{3}{2}} \left[\frac{1}{2}\hat{\xi}_M(\hat{p}_1 - \hat{p}_2) - (p\xi_M) \right] |p|^{-1} \\ ^1P_1 & \sqrt{3}(p\xi_M)|p|^{-1}\end{array}$$

There are eight states in the deuteron channel (instead of two in the non-relativistic case), viz. $^3S_1^{++}$, $^3D_1^{++}$, $^3S_1^{--}$, $^3D_1^{--}$, $^3P_1^e$, $^3P_1^o$, $^1P_1^e$, $^1P_1^o$ (notation: $2S+1 L_J^{\rho_1 \rho_2}$). The normalization condition for these functions can be written as:

$$\begin{aligned}P_+ + P_- &= 1, & P_+ &= P_{^3S_1^{++}} + P_{^3D_1^{++}}, \\ P_- &= P_{^3S_1^{--}} + P_{^3D_1^{--}} + P_{^3P_1^e} + P_{^3P_1^o} + P_{^1P_1^e} + P_{^1P_1^o},\end{aligned}\quad (4)$$

introducing pseudo-probabilities P_α that are negative for the states $^3S_1^{--}$, $^3D_1^{--}$, $^3P_1^e$, $^3P_1^o$, $^1P_1^e$, $^1P_1^o$, and positive for $^3S_1^{++}$, $^3D_1^{++}$ (Ref.[3]). The calculations with realistic vertex functions give the following values:

	$^3D_1^{++}$	$^3D_1^{--}$	$^3P_1^e + ^3P_1^o$	$^1P_1^e + ^1P_1^o$	
[%]	4.8	$-6 \cdot 10^{-4}$	$-0.88 \cdot 10^{-2}$	$-2.5 \cdot 10^{-2}$	Ref.[3]
[%]	5.1	$-3.4 \cdot 10^{-4}$	$-9 \cdot 10^{-2}$	$-2.4 \cdot 10^{-2}$	Ref.[5]

It is obvious that the main contribution to the normalization is due to the states with positive energies, and the contribution of the P -states is larger than that of the negative energy states by at least one order of magnitude.

3 The calculation of the magnetic moment

The matrix element of the electromagnetic current to evaluate the magnetic moment of the deuteron is given by

$$\langle P' M' | J_x | PM \rangle = \frac{ie}{2\pi^2 M} \int d^4 p$$

$$Tr \left\{ \bar{\Gamma}_{M'}(P', p') S^{(1)} \left(\frac{P'}{2} + p' \right) [\gamma_1 F_1^{(s)}(q^2) - \frac{\gamma_1 \hat{q} - \hat{q} \gamma_1}{4m} F_2^{(s)}(q^2)] \Psi_M(P, p) \right\}, \quad (5)$$

where $\Psi_M(P, p) = S^{(1)} \left(\frac{P}{2} + p \right) \Gamma_M(P, p) \tilde{S}^{(2)} \left(\frac{P}{2} - p \right)$, the isoscalar form factors of the nucleons are given by $F_{1,2}^{(s)}(q^2)$, and $p' = p + q/2$, $P' = P + q$. The magnetic moment then is evaluated via

$$\mu_D = \frac{1}{e} \frac{m}{M} \sqrt{2} \lim_{\eta \rightarrow 0} \frac{\langle M' = +1 | J_x | M = 0 \rangle}{\sqrt{\eta} \sqrt{1 + \eta}}, \quad (6)$$

with $\eta = -q^2/4M^2$. Since the integral (5) vanishes at $q^2 = 0$, we expand the integrand of (5) in powers of $\sqrt{\eta}$. This is done in the Breit system. Hence the vertex functions should be transformed from the rest system to the Breit system using the following formulae

$$\begin{aligned}\Gamma_M(P^{(B)}, p^{(B)}) &= \Lambda(P^{(B)}) \Gamma_M(P^{(0)}, p^{(0)}) \Lambda^{-1}(P^{(B)}), \\ \Gamma_M(P'^{(B)}, p'^{(B)}) &= \Lambda^{-1}(P^{(B)}) \Gamma_M(P^{(0)}, p^{(0)}) \Lambda(P^{(B)}),\end{aligned}$$

where $\Lambda(P^{(B)}) = (M + \hat{P}^{(B)}\gamma_0)/\sqrt{2M(E^{(B)} + M)}$, and the vectors $P^{(B)}, P'^{(B)}$, $p^{(B)}, p'^{(B)}$ are connected with the respective vectors in the rest system by the Lorentz transformation (7) $P^{(B)} = \mathcal{L}P^{(0)}$, $p^{(B)} = \mathcal{L}p^{(0)}$, $P'^{(B)} = \mathcal{L}^{-1}P^{(0)}$, $p'^{(B)} = \mathcal{L}^{-1}p^{(0)}$. (7)

The Lorentz transformation matrix \mathcal{L} is of the form

$$\mathcal{L} = \begin{pmatrix} \sqrt{1+\eta} & 0 & 0 & -\sqrt{\eta} \\ 0 & 1 & 0 & 0 \\ 0 & 0 & 1 & 0 \\ -\sqrt{\eta} & 0 & 0 & \sqrt{1+\eta} \end{pmatrix} \quad (8)$$

From (7) it follows that $p'^{(0)} = \mathcal{L}p'^{(B)} = \mathcal{L}(p^{(B)} + \frac{1}{2}\mathcal{L}q^{(B)}) = \mathcal{L}^2 p^{(0)} + \frac{1}{2}\mathcal{L}q^{(B)}$. To simplify notation the vector $p^{(0)}$ will be denoted as $p^{(0)} \equiv p = (p_0, p_x, p_y, p_z)$.

The components of the vector $p'^{(0)} \equiv p'$ are then given by

$$\begin{aligned}p'_0 &= (1 + 2\eta)p_0 + 2\sqrt{\eta}\sqrt{1 + \eta}p_z - M\eta, \\ p'_x &= p_x, \quad p'_y = p_y, \\ p'_z &= (1 + 2\eta)p_z - 2\sqrt{\eta}\sqrt{1 + \eta}p_0 + M\sqrt{\eta}\sqrt{1 + \eta}.\end{aligned}\quad (9)$$

With the help of the transformations (7), the integral (5) may then be written as

$$\begin{aligned}\langle P' M' | J_x | PM \rangle &= \frac{ie}{2\pi^2 M} \int d^4 p Tr \left\{ \bar{\Gamma}_{M'}(P^{(0)}, p') S^{(1)} \left(\frac{P^{(0)}}{2} + p' \right) \Lambda(P^{(B)}) \right. \\ &\quad \left. [\gamma_1 F_1^{(s)}(q^2) - \frac{\gamma_1 \hat{q} - \hat{q} \gamma_1}{4m} F_2^{(s)}(q^2)] \Lambda(P^{(B)}) \Psi_M(P^{(0)}, p) [\Lambda^{-1}(P^{(B)})]^2 \right\},\end{aligned}\quad (10)$$

where the wave function $\Psi_M(P^{(0)}, p)$ and the vertex function $\bar{\Gamma}_{M'}(P^{(0)}, p')$ are taken in the deuteron rest frame.

It is obvious from (10) that the sources of $\sqrt{\eta}$ terms may appear in (i) the matrix $\Lambda(P^{(B)})$, (ii) the propagator $S^{(1)}(\frac{1}{2}P^{(0)} + p')$, and (iii) the vertex function $\bar{\Gamma}_{M'}(P^{(0)}, p')$. In detail this reads for the matrix (i)

$$\begin{aligned}\Lambda(P^{(B)}) & [\gamma_1 F_1^{(s)}(q^2) - \frac{\gamma_1 \hat{q} - \hat{q}\gamma_1}{4m} F_2^{(s)}(q^2)] \Lambda(P^{(B)}) = \\ & = \frac{1}{2} (\gamma_1 + \sqrt{\eta} \gamma_1 \gamma_3 \gamma_0 - \frac{\kappa}{4m} (\gamma_1 \hat{q} - \hat{q}\gamma_1)),\end{aligned}\quad (11)$$

and for the propagator (ii) $[\Lambda^{-1}(P^{(B)})]^2 = 1 + \sqrt{\eta} \gamma_0 \gamma_3$, and for the vertex function (iii)

$$\begin{aligned}S^{(1)}\left(\frac{P^{(0)}}{2} + p'\right) &= S^{(1)}\left(\frac{P^{(0)}}{2} + p\right) \left[1 + \sqrt{\eta} \frac{4M p_z \gamma_0}{(\frac{P^{(0)}}{2} + p)^2 - m^2} \right] - \\ &\quad \sqrt{\eta} \frac{2p_z \gamma_0 + (M - 2p_0)\gamma_3}{(\frac{P^{(0)}}{2} + p)^2 - m^2}.\end{aligned}\quad (12)$$

The corrections due to the vertex function (iii) may be separated into (α) corrections due to the radial wave functions, and (β) due to the spin – angular momentum function. This will be demonstrated in the following using only one component of the vertex function (2), i.e.

$$\bar{\Gamma}_{M'}(P^{(0)}, p') = g(p'_0, |p'|) \bar{\Gamma}_{M'}(p').\quad (13)$$

For the radial part we get the following expansion

$$g(p'_0, |p'|) = g(p_0, |p|) + \sqrt{\eta} p_z \left\{ -2 \frac{\partial}{\partial p_0} + \frac{M - 2p_0}{|p|} \frac{\partial}{\partial |p|} \right\} g(p_0, |p|).\quad (14)$$

The spin – angular momentum part can be written (e.g. for the ${}^3D_1^{++}$ state) as

$$\bar{\Gamma}_{M'}(p) = N(E')(m - \hat{p}'_1) \bar{\Gamma}(p', \xi)(m + \hat{p}'_2),\quad (15)$$

where

$$\hat{p}'_1 = \hat{p}_1 + \sqrt{\eta} (M - 2p_0) \left[\frac{p_z}{E} \gamma_0 - \gamma_3 \right],\quad (16)$$

$$\hat{p}'_2 = \hat{p}_2 + \sqrt{\eta} (M - 2p_0) \left[\frac{p_z}{E} \gamma_0 + \gamma_3 \right].\quad (17)$$

$$\begin{aligned}N(E') &= \frac{1}{2E'(m + E')} = \\ &= \frac{1}{2E(m + E)} \left(1 - \sqrt{\eta} \frac{M - 2p_0}{E^2(m + E)} (m + 2E)p_z \right),\end{aligned}\quad (17)$$

and corrections to $\bar{\Gamma}(p', \xi)$ can be calculated using (16)–(17).

4 Results of calculations

The general formula for magnetic moment can be written as

$$\begin{aligned}\mu &= \mu_+ + \mu_{1-} + \mu_{2-} + \mu_3, \\ \mu_+ &= (\mu_p + \mu_n)(P_3 S_1^{++} + P_3 D_1^{++}) - \frac{3}{2} (\mu_p + \mu_n - \frac{1}{2}) P_3 D_1^{++} + R_+, \\ \mu_{1-} &= \frac{1}{2} (\mu_p + \mu_n)(P_3 P_1^e + P_3 P_1^o) + \\ &\quad + \frac{1}{4} (P_3 P_1^e + P_3 P_1^o) + \frac{1}{2} (P_1 P_1^e + P_1 P_1^o) + R_{1-},\end{aligned}$$

$$\begin{aligned}\mu_{2-} &= -(\mu_p + \mu_n) P_3 S_1^{--} + P_3 S_1^{+-} + \frac{1}{2} (\mu_p + \mu_n) P_3 D_1^{--} - \frac{5}{4} P_3 D_1^{+-} + R_{2-}, \\ \mu_3 &= C^3 S_1^{++}, {}^1P_1^e + C^3 S_1^{++}, {}^1P_1^o + C^3 S_1^{++}, {}^3P_1^e + C^3 S_1^{++}, {}^3P_1^o + \\ &\quad + C^3 S_1^{--}, {}^1P_1^e + C^3 S_1^{--}, {}^1P_1^o + C^3 S_1^{--}, {}^3P_1^e + C^3 S_1^{--}, {}^3P_1^o + \\ &\quad + C^3 D_1^{++}, {}^1P_1^e + C^3 D_1^{++}, {}^1P_1^o + C^3 D_1^{++}, {}^3P_1^e + C^3 D_1^{++}, {}^3P_1^o + \\ &\quad + C^3 D_1^{--}, {}^1P_1^e + C^3 D_1^{--}, {}^1P_1^o + C^3 D_1^{--}, {}^3P_1^e + C^3 D_1^{--}, {}^3P_1^o,\end{aligned}$$

where R_a are the relativistic correction terms, viz.

$$\begin{aligned}R_+ &= -\frac{1}{3} (\mu_p + \mu_n - 1 + \frac{2m}{M}) H_1^3 S_1^{++} - \frac{m}{M} H_2^3 S_1^{++} - \frac{m}{M} H_3^3 S_1^{++} - \\ &\quad - (1 - \frac{2m}{M}) P_3 S_1^{++} - \frac{1}{6} (\mu_p + \mu_n - 1 - \frac{4m}{M}) H_1^3 D_1^{++} - \\ &\quad - \frac{m}{M} H_2^3 D_1^{++} - \frac{m}{M} H_3^3 D_1^{++} - \frac{1}{4} (1 - \frac{2m}{M}) P_3 D_1^{++} + \\ &\quad + \frac{\sqrt{2}}{3} (\mu_p + \mu_n - 1 - \frac{m}{M}) H_1^3 S_1^{++}, {}^3D_1^{++}, \\ R_{1-} &= -\frac{1}{2} (1 - \frac{2m}{M}) (\mu_p + \mu_n + \frac{1}{2}) (P_3 P_1^e + P_3 P_1^o) - \\ &\quad - \frac{1}{2} (1 - \frac{2m}{M}) (P_1 P_1^e + P_1 P_1^o) + (\mu_p + \mu_n + 1) H_4^3 P_1^e, {}^3P_1^o + \\ &\quad + 2H_4^1 P_1^e, {}^1P_1^o + 2\sqrt{2} \frac{m}{M} (H_4^3 P_1^e, {}^1P_1^e + H_4^3 P_1^o, {}^1P_1^o) + \\ &\quad + \sqrt{2} (\mu_p + \mu_n - 1 + \frac{4m^2}{M^2}) H_5^3 P_1^e, {}^1P_1^o + \sqrt{2} (\mu_p + \mu_n - 1) H_5^3 P_1^o, {}^1P_1^e - \\ &\quad - \frac{\sqrt{2}}{2} H_6^3 P_1^e, {}^1P_1^e - 2\sqrt{2} \frac{m}{M} H_7^3 P_1^o, {}^1P_1^e, \\ R_{2-} &= -\frac{1}{3} (\mu_p + \mu_n - 1 - \frac{2m}{M}) H_1^3 S_1^{--} - \frac{m}{M} H_2^3 S_1^{--} + \frac{m}{M} H_3^3 S_1^{--} + \\ &\quad - \frac{1}{6} (\mu_p + \mu_n - 1 + \frac{4m}{M}) H_1^3 D_1^{--} - \frac{m}{M} H_2^3 D_1^{--} + \frac{m}{M} H_3^3 D_1^{--} + \\ &\quad + \frac{3}{4} (1 - \frac{2m}{M}) P_3 D_1^{--} + \frac{\sqrt{2}}{3} (\mu_p + \mu_n - 1 + \frac{m}{M}) H_1^3 S_1^{--}, {}^3D_1^{--},\end{aligned}$$

quantities $C^{\alpha, \alpha'}$ are

$$C^{3S_1^{++}, 1P_1^*} = \frac{\sqrt{6}}{12M} \left[G_1^{3S_1^{++}, 1P_1^*} + 4G_2^{3S_1^{++}, 1P_1^*} - 4G_3^{3S_1^{++}, 1P_1^*} - G_4^{3S_1^{++}, 1P_1^*} - 4G_5^{3S_1^{++}, 1P_1^*} \right],$$

$$C^{3S_1^{--}, 1P_1^*} = \frac{\sqrt{6}}{12M} \left[G_1^{3S_1^{--}, 1P_1^*} + 4G_2^{3S_1^{--}, 1P_1^*} - 4G_3^{3S_1^{--}, 1P_1^*} - G_4^{3S_1^{--}, 1P_1^*} - 4G_5^{3S_1^{--}, 1P_1^*} \right],$$

$$C^{3S_1^{++}, 3P_1^*} = \frac{\sqrt{6}}{3M} \left[-G_6^{3S_1^{++}, 3P_1^*} - G_7^{3S_1^{++}, 3P_1^*} - G_8^{3S_1^{++}, 3P_1^*} \right],$$

$$C^{3S_1^{--}, 3P_1^*} = \frac{\sqrt{6}}{3M} \left[G_6^{3S_1^{--}, 3P_1^*} + G_7^{3S_1^{--}, 3P_1^*} + G_8^{3S_1^{--}, 3P_1^*} \right],$$

$$C^{3D_1^{++}, 1P_1^*} = \frac{\sqrt{3}}{60M} \left[G_9^{3D_1^{++}, 1P_1^*} + 4G_{10}^{3D_1^{++}, 1P_1^*} - 8G_{11}^{3D_1^{++}, 1P_1^*} - 2G_{12}^{3D_1^{++}, 1P_1^*} - 8G_{13}^{3D_1^{++}, 1P_1^*} \right],$$

$$C^{3D_1^{--}, 1P_1^*} = \frac{\sqrt{3}}{60M} \left[G_9^{3D_1^{--}, 1P_1^*} + 4G_{10}^{3D_1^{--}, 1P_1^*} - 8G_{11}^{3D_1^{--}, 1P_1^*} - 2G_{12}^{3D_1^{--}, 1P_1^*} - 8G_{13}^{3D_1^{--}, 1P_1^*} \right],$$

$$C^{3D_1^{++}, 3P_1^*} = \frac{\sqrt{3}}{15M} \left[-G_{14}^{3D_1^{++}, 3P_1^*} + 2G_{15}^{3D_1^{++}, 3P_1^*} - G_{16}^{3D_1^{++}, 3P_1^*} - 2G_{17}^{3D_1^{++}, 3P_1^*} \right],$$

$$C^{3D_1^{--}, 3P_1^*} = \frac{\sqrt{3}}{15M} \left[-G_{14}^{3D_1^{--}, 3P_1^*} - 2G_{15}^{3D_1^{--}, 3P_1^*} + G_{16}^{3D_1^{--}, 3P_1^*} + 2G_{17}^{3D_1^{--}, 3P_1^*} \right],$$

$$C^{3S_1^{++}, 3P_1^*} = \frac{\sqrt{3}}{3} \left[\frac{m}{M} \left(G_{18}^{3S_1^{++}, 3P_1^*} - G_7^{3S_1^{++}, 3P_1^*} - G_8^{3S_1^{++}, 3P_1^*} \right) - \kappa G_{19}^{3S_1^{++}, 3P_1^*} \right],$$

$$C^{3S_1^{--}, 3P_1^*} = \frac{\sqrt{3}}{3} \left[-\frac{m}{M} \left(G_{18}^{3S_1^{--}, 3P_1^*} + G_7^{3S_1^{--}, 3P_1^*} + G_8^{3S_1^{--}, 3P_1^*} \right) - \kappa G_{19}^{3S_1^{--}, 3P_1^*} \right],$$

$$C^{3S_1^{++}, 3P_1^*} = \frac{\sqrt{3}}{3} \left[-\frac{m}{M} \left(G_{20}^{3S_1^{++}, 3P_1^*} + G_{21}^{3S_1^{++}, 3P_1^*} + G_3^{3S_1^{++}, 3P_1^*} + \frac{1}{4} G_4^{3S_1^{++}, 3P_1^*} + G_5^{3S_1^{++}, 3P_1^*} \right) - \kappa G_{22}^{3S_1^{++}, 3P_1^*} \right],$$

$$C^{3S_1^{--}, 3P_1^*} = \frac{\sqrt{3}}{3} \left[\frac{m}{M} \left(G_{20}^{3S_1^{--}, 3P_1^*} + G_{21}^{3S_1^{--}, 3P_1^*} + G_3^{3S_1^{--}, 3P_1^*} + \frac{1}{4} G_4^{3S_1^{--}, 3P_1^*} + G_5^{3S_1^{--}, 3P_1^*} \right) + \kappa G_{22}^{3S_1^{--}, 3P_1^*} \right],$$

$$C^{3D_1^{++}, 3P_1^*} = \frac{\sqrt{6}}{3} \left[\frac{m}{M} \left(G_{23}^{3D_1^{++}, 3P_1^*} - G_{24}^{3D_1^{++}, 3P_1^*} - G_7^{3D_1^{++}, 3P_1^*} - G_8^{3D_1^{++}, 3P_1^*} \right) + \frac{1}{2} \kappa G_{19}^{3D_1^{++}, 3P_1^*} \right],$$

$$C^{3D_1^{--}, 3P_1^*} = \frac{\sqrt{6}}{3} \left[-\frac{m}{M} \left(G_{23}^{3D_1^{--}, 3P_1^*} + G_{24}^{3D_1^{--}, 3P_1^*} + G_7^{3D_1^{--}, 3P_1^*} + G_8^{3D_1^{--}, 3P_1^*} \right) + \frac{1}{2} \kappa G_{19}^{3D_1^{--}, 3P_1^*} \right],$$

$$C^{3D_1^{++}, 3P_1^*} = \frac{\sqrt{6}}{3} \left[\frac{m}{M} \left(G_{25}^{3D_1^{++}, 3P_1^*} + G_{26}^{3D_1^{++}, 3P_1^*} + G_3^{3D_1^{++}, 3P_1^*} + \frac{1}{4} G_4^{3D_1^{++}, 3P_1^*} + G_5^{3D_1^{++}, 3P_1^*} \right) + \frac{1}{2} \kappa G_{22}^{3D_1^{++}, 3P_1^*} \right],$$

$$+ \frac{1}{2} \kappa G_{22}^{3D_1^{++}, 3P_1^*} \Bigg],$$

$$C^{3D_1^{--}, 3P_1^*} = \frac{\sqrt{6}}{3} \left[\frac{m}{M} \left(G_{25}^{3D_1^{--}, 3P_1^*} + G_{26}^{3D_1^{--}, 3P_1^*} + G_3^{3D_1^{--}, 3P_1^*} + \frac{1}{4} G_4^{3D_1^{--}, 3P_1^*} + G_5^{3D_1^{--}, 3P_1^*} \right) - \frac{1}{2} \kappa G_{22}^{3D_1^{--}, 3P_1^*} \right],$$

and $H_i^{\alpha, \alpha'} (H_i^{\alpha, \alpha} \equiv H_i^\alpha)$ and $G^{\alpha, \alpha'}$ are integrals of the form $\frac{-i}{4\pi^2 M} \int dp_0 |\mathbf{p}|^2 d|\mathbf{p}|$ with the integrands given by (compare with Ref.[6])

$$H_1^{\alpha, \alpha'} = \left(\frac{E-m}{E} \right) [\phi_\alpha(p_0, |\mathbf{p}|) \phi_{\alpha'}(p_0, |\mathbf{p}|)] \begin{cases} (E-M/2), \text{ for } \alpha(\alpha') = {}^3S_1^{++}, {}^3D_1^{++}, \\ (E+M/2), \text{ for } \alpha(\alpha') = {}^3S_1^{--}, {}^3D_1^{--} \end{cases}$$

$$H_2^{\alpha, \alpha'} = \left(\frac{E-M/2}{E} \right) [\phi_\alpha(p_0, |\mathbf{p}|) \phi_{\alpha'}(p_0, |\mathbf{p}|)] \begin{cases} (E-M/2), \text{ for } \alpha(\alpha') = {}^3S_1^{++}, {}^3D_1^{++}, \\ (E+M/2), \text{ for } \alpha(\alpha') = {}^3S_1^{--}, {}^3D_1^{--} \end{cases}$$

$$H_3^{\alpha, \alpha'} = \left(\frac{p_0^2}{E} \right) [\phi_\alpha(p_0, |\mathbf{p}|) \phi_{\alpha'}(p_0, |\mathbf{p}|)], \quad H_4^{\alpha, \alpha'} = \left(\frac{m}{E} p_0 \right) [\phi_\alpha(p_0, |\mathbf{p}|) \phi_{\alpha'}(p_0, |\mathbf{p}|)]$$

$$H_5^{\alpha, \alpha'} = \left(-\frac{M}{2} \right) [\phi_\alpha(p_0, |\mathbf{p}|) \phi_{\alpha'}(p_0, |\mathbf{p}|)], \quad H_6^{\alpha, \alpha'} = \left(\frac{m^2}{E^2} M \right) [\phi_\alpha(p_0, |\mathbf{p}|) \phi_{\alpha'}(p_0, |\mathbf{p}|)]$$

$$H_7^{\alpha, \alpha'} = \left(\frac{m}{E^2} p_0^2 \right) [\phi_\alpha(p_0, |\mathbf{p}|) \phi_{\alpha'}(p_0, |\mathbf{p}|)],$$

$$G_1^{\alpha, \alpha'} = \frac{(E-m)Mm}{|\mathbf{p}|E^2} [\phi_\alpha(p_0, |\mathbf{p}|) \phi_{\alpha'}(p_0, |\mathbf{p}|)] \begin{cases} (M-2E), \text{ for } \alpha = {}^3S_1^{++}, {}^3D_1^{++}, \\ (M+2E), \text{ for } \alpha = {}^3S_1^{--}, {}^3D_1^{--} \end{cases}$$

$$G_2^{\alpha, \alpha'} = \frac{(E-m)m}{|\mathbf{p}|E^2} p_0^2 [\phi_\alpha(p_0, |\mathbf{p}|) \phi_{\alpha'}(p_0, |\mathbf{p}|)], \quad G_3^{\alpha, \alpha'} = |\mathbf{p}| p_0 \left[\frac{\partial}{\partial p_0} \phi_\alpha(p_0, |\mathbf{p}|) \phi_{\alpha'}(p_0, |\mathbf{p}|) \right],$$

$$G_4^{\alpha, \alpha'} = M \left[\frac{\partial}{\partial |\mathbf{p}|} \phi_\alpha(p_0, |\mathbf{p}|) \phi_{\alpha'}(p_0, |\mathbf{p}|) \right] \begin{cases} (M-2E), \text{ for } \alpha = {}^3S_1^{++}, {}^3D_1^{++}, \\ (M+2E), \text{ for } \alpha = {}^3S_1^{--}, {}^3D_1^{--}, \end{cases}$$

$$G_5^{\alpha, \alpha'} = p_0^2 \left[\frac{\partial}{\partial |\mathbf{p}|} \phi_\alpha(p_0, |\mathbf{p}|) \phi_{\alpha'}(p_0, |\mathbf{p}|) \right],$$

$$G_6^{\alpha, \alpha'} = \frac{E-m}{|\mathbf{p}|E} p_0 [\phi_\alpha(p_0, |\mathbf{p}|) \phi_{\alpha'}(p_0, |\mathbf{p}|)] \begin{cases} (M+m), \text{ for } \alpha = {}^3S_1^{++}, {}^3D_1^{++}, \\ (M-m), \text{ for } \alpha = {}^3S_1^{--}, {}^3D_1^{--} \end{cases}$$

$$G_7^{\alpha, \alpha'} = \frac{|\mathbf{p}|}{2} \left[\frac{\partial}{\partial p_0} \phi_\alpha(p_0, |\mathbf{p}|) \phi_{\alpha'}(p_0, |\mathbf{p}|) \right] \begin{cases} (M-2E), \text{ for } \alpha = {}^3S_1^{++}, {}^3D_1^{++}, \\ (M+2E), \text{ for } \alpha = {}^3S_1^{--}, {}^3D_1^{--}, \end{cases}$$

$$G_8^{\alpha, \alpha'} = p_0 \left[\frac{\partial}{\partial |\mathbf{p}|} \phi_\alpha(p_0, |\mathbf{p}|) \phi_{\alpha'}(p_0, |\mathbf{p}|) \right] \begin{cases} (M-2E), \text{ for } \alpha = {}^3S_1^{++}, {}^3D_1^{++}, \\ (M+E), \text{ for } \alpha = {}^3S_1^{--}, {}^3D_1^{--}, \end{cases}$$

$$G_9^{\alpha, \alpha'} = \frac{E^2 + 4mE + m^2}{|\mathbf{p}|E^2} M [\phi_\alpha(p_0, |\mathbf{p}|) \phi_{\alpha'}(p_0, |\mathbf{p}|)] \begin{cases} (M-2E), \text{ for } \alpha = {}^3S_1^{++}, {}^3D_1^{++}, \\ (M+2E), \text{ for } \alpha = {}^3S_1^{--}, {}^3D_1^{--}, \end{cases}$$

$$G_{10}^{\alpha, \alpha'} = \frac{E^2 + 4mE + m^2}{|\mathbf{p}|E^2} p_0^2 [\phi_\alpha(p_0, |\mathbf{p}|) \phi_{\alpha'}(p_0, |\mathbf{p}|)],$$

$$G_{11}^{\alpha, \alpha'} = \frac{m-2E}{E} |\mathbf{p}| p_0 \left[\frac{\partial}{\partial p_0} \phi_\alpha(p_0, |\mathbf{p}|) \phi_{\alpha'}(p_0, |\mathbf{p}|) \right],$$

$$\begin{aligned}
G_{12}^{\alpha, \alpha'} &= \frac{m-2E}{E} M \left[\frac{\partial}{\partial |\mathbf{p}|} \phi_\alpha(p_0, |\mathbf{p}|) \phi_{\alpha'}(p_0, |\mathbf{p}|) \right] \begin{cases} (M-2E), \text{ for } \alpha = {}^3S_1^{++}, {}^3D_1^{++} \\ (M+2E), \text{ for } \alpha = {}^3S_1^{--}, {}^3D_1^{--} \end{cases} \\
G_{13}^{\alpha, \alpha'} &= \frac{m-2E}{E} p_0^2 \left[\frac{\partial}{\partial |\mathbf{p}|} \phi_\alpha(p_0, |\mathbf{p}|) \phi_{\alpha'}(p_0, |\mathbf{p}|) \right], \\
G_{14}^{\alpha, \alpha'} &= \frac{E^2 + 4mE + m^2}{|\mathbf{p}|E} p_0 \left[\phi_\alpha(p_0, |\mathbf{p}|) \phi_{\alpha'}(p_0, |\mathbf{p}|) \right], \\
G_{15}^{\alpha, \alpha'} &= \frac{E^3 + 3mE^2 - m^3}{|\mathbf{p}|E^3} M p_0 \left[\phi_\alpha(p_0, |\mathbf{p}|) \phi_{\alpha'}(p_0, |\mathbf{p}|) \right], \\
G_{16}^{\alpha, \alpha'} &= \frac{m-2E}{E} |\mathbf{p}| \left[\frac{\partial}{\partial p_0} \phi_\alpha(p_0, |\mathbf{p}|) \phi_{\alpha'}(p_0, |\mathbf{p}|) \right] \begin{cases} (M-2E), \text{ for } \alpha = {}^3S_1^{++}, {}^3D_1^{++} \\ (M+2E), \text{ for } \alpha = {}^3S_1^{--}, {}^3D_1^{--} \end{cases} \\
G_{17}^{\alpha, \alpha'} &= \frac{m-2E}{E} p_0 \left[\frac{\partial}{\partial |\mathbf{p}|} \phi_\alpha(p_0, |\mathbf{p}|) \phi_{\alpha'}(p_0, |\mathbf{p}|) \right] \begin{cases} (M-E), \text{ for } \alpha = {}^3S_1^{++}, {}^3D_1^{++} \\ (M+E), \text{ for } \alpha = {}^3S_1^{--}, {}^3D_1^{--} \end{cases} \\
G_{18}^{\alpha, \alpha'} &= \frac{E-m}{|\mathbf{p}|E} p_0 \left[\phi_\alpha(p_0, |\mathbf{p}|) \phi_{\alpha'}(p_0, |\mathbf{p}|) \right] \begin{cases} (E-2M-m), \text{ for } \alpha = {}^3S_1^{++}, {}^3D_1^{++} \\ (E+2M-m), \text{ for } \alpha = {}^3S_1^{--}, {}^3D_1^{--} \end{cases} \\
G_{19}^{\alpha, \alpha'} &= \frac{|\mathbf{p}|}{E} p_0 \left[\phi_\alpha(p_0, |\mathbf{p}|) \phi_{\alpha'}(p_0, |\mathbf{p}|) \right], \\
G_{20}^{\alpha, \alpha'} &= \frac{(E-m)^2}{4|\mathbf{p}|E^2} M \left[\phi_\alpha(p_0, |\mathbf{p}|) \phi_{\alpha'}(p_0, |\mathbf{p}|) \right] \begin{cases} (M-2E), \text{ for } \alpha = {}^3S_1^{++}, {}^3D_1^{++} \\ (M+2E), \text{ for } \alpha = {}^3S_1^{--}, {}^3D_1^{--} \end{cases} \\
G_{21}^{\alpha, \alpha'} &= \frac{(E-m)^2}{|\mathbf{p}|E^2} p_0^2 \left[\phi_\alpha(p_0, |\mathbf{p}|) \phi_{\alpha'}(p_0, |\mathbf{p}|) \right], \\
G_{22}^{\alpha, \alpha'} &= \frac{|\mathbf{p}|}{2E} \left[\phi_\alpha(p_0, |\mathbf{p}|) \phi_{\alpha'}(p_0, |\mathbf{p}|) \right] \begin{cases} (M-2E), \text{ for } \alpha = {}^3S_1^{++}, {}^3D_1^{++} \\ (M+2E), \text{ for } \alpha = {}^3S_1^{--}, {}^3D_1^{--} \end{cases} \\
G_{23}^{\alpha, \alpha'} &= \frac{E^2 + mE + m^2}{|\mathbf{p}|E} p_0 \left[\phi_\alpha(p_0, |\mathbf{p}|) \phi_{\alpha'}(p_0, |\mathbf{p}|) \right], \\
G_{24}^{\alpha, \alpha'} &= \frac{m+2E}{|\mathbf{p}|E} M p_0 \left[\phi_\alpha(p_0, |\mathbf{p}|) \phi_{\alpha'}(p_0, |\mathbf{p}|) \right], \\
G_{25}^{\alpha, \alpha'} &= \frac{E^2 + mE + m^2}{4|\mathbf{p}|E^2} M \left[\phi_\alpha(p_0, |\mathbf{p}|) \phi_{\alpha'}(p_0, |\mathbf{p}|) \right] \begin{cases} (M-2E), \text{ for } \alpha = {}^3S_1^{++}, {}^3D_1^{++} \\ (M+2E), \text{ for } \alpha = {}^3S_1^{--}, {}^3D_1^{--} \end{cases}, \\
G_{26}^{\alpha, \alpha'} &= \frac{E^2 + mE + m^2}{|\mathbf{p}|E^2} p_0^2 \left[\phi_\alpha(p_0, |\mathbf{p}|) \phi_{\alpha'}(p_0, |\mathbf{p}|) \right]
\end{aligned}$$

The relativistic corrections R_α can be estimated numerically for a separable model [7]. They are smaller than the dominant terms by at least one order of magnitude. Taking into account different orders of pseudo-probabilities one gets

$$\mu_d = \mu_{NR} + \Delta\mu, \quad (18)$$

$$\mu_{NR} = (\mu_p + \mu_n) - \frac{3}{2}(\mu_p + \mu_n - \frac{1}{2})P_3 D_1^{++}, \quad \Delta\mu = R_+ + \Delta\mu_{1-},$$

$$\Delta\mu_{1-} = -\frac{1}{2}(\mu_p + \mu_n)(P_3 P_1^e + P_3 P_1^o) - (\mu_p + \mu_n)(P_1 P_1^e + P_1 P_1^o)$$

$$+ \frac{1}{4}(P_3 P_1^e + P_3 P_1^o) + \frac{1}{2}(P_1 P_1^e + P_1 P_1^o) \quad (19)$$

The contribution R_+ is negative and $\Delta\mu_{1-}$ is positive. An estimation gives the following results

$$R_+/\mu_{NR} = -(5.8 - 11) \times 10^{-2} \%, \quad \Delta\mu_{1-}/\mu_{NR} = (0.01 - 0.03) \% \quad (19)$$

5 Conclusion

We have shown that the expression for the magnetic moment in the Bethe-Salpeter approach can be written in a form closer to non-relativistic calculations. The additional terms in equation (18) can be considered as relativistic corrections to the non-relativistic formula.

The experimental value of the magnetic moment is known with a high accuracy: $\mu_{exp} = 0.857406(1)$. The non-relativistic value reflects only the D -state probability. Whereas in the relativistic corrections P -states play the dominant role.

The magnitude of the corrections can be compared with the contributions of mesonic exchange currents to the magnetic moment as extracted from Ref.[8]. The main contribution is due to the pair term, which leads to $\Delta\mu/\mu_{NR} = 0.21 - 0.22\%$ for different forms of the Bonn potential. The close size of this correction as compared to (19) may be considered as an indication that both corrections are of the same physical origin.

6 Acknowledgements

This work has been partially supported by the Deutsche Akademische Austauschdienst and by the Russian Foundation for Fundamental Researches Grant № 94-02-05005.

References

- [1] E.E.Salpeter and H.A.Bethe, *Phys. Rev.* **C84** (1951) 1232.
- [2] B.Desplanques *et al.*, *preprint IPNO/TH 94-78*.
- [3] M.J.Zuilhof, J.A.Tjon, *Phys.Rev.* **C22** (1980) 2369.
- [4] J.J.Kubis, *Phys. Rev.* **D6** (1972) 547.
- [5] K.Kazakov, *private communication*. We are grateful to K.Kazakov for providing us with this numbers prior to publication.
- [6] N.Honzava, S.Ishida, *Phys. Rev.* **C45** (1992) 47.

- [7] G.Rupp, J.A.Tjon, *Phys. Rev. C* **37** (1988) 1729.
- [8] V.V.Burov, V.N.Dostovalov, S.E.Suskov, *Fiz. Elem. Chastits At. Yadra* **23** (1992) 721 [*Sov. J. Part. Nucl.* **23** (1992) 317].

Received by Publishing Department
on October 24, 1995.